6-10-2015

Repulsive Casimir force between Weyl semimetals

Justin H. Wilson
University of Maryland, College Park

Andrew A. Allocca
University of Maryland, College Park

Victor Galitski
University of Maryland, College Park

Recommended Citation

Wilson, J., Allocca, A., & Galitski, V. (2015). Repulsive Casimir force between Weyl semimetals. *Physical Review B - Condensed Matter and Materials Physics, 91* (23) https://doi.org/10.1103/PhysRevB.91.235115

Repulsive Casimir force between Weyl semimetals

Justin H. Wilson, Andrew A. Allocca, and Victor Galitski

Phys. Rev. B **91**, 235115 — Published 10 June 2015

DOI: 10.1103/PhysRevB.91.235115

Repulsive Casimir force between Weyl semimetals

Justin H. Wilson,[1,2] Andrew A. Allocca,[1] and Victor Galitski[1,2]

[1] *Joint Quantum Institute and Condensed Matter Theory Center, Department of Physics, University of Maryland, College Park, Maryland 20742-4111, USA*
[2] *School of Physics, Monash University, Melbourne, Victoria 3800, Australia*

Weyl semimetals are a class of topological materials that exhibit a bulk Hall effect due to time-reversal symmetry breaking. We show that for the idealized semi-infinite case, the Casimir force between two identical Weyl semimetals is repulsive at short range and attractive at long range. Considering plates of finite thickness, we can reduce the size of the long-range attraction even making it repulsive for all distances when thin enough. In the thin film limit, we study the appearance of an attractive Casimir force at shorter distances due to the longitudinal conductivity. Magnetic field, thickness, and chemical potential provide tunable nobs for this effect, controlling the Casimir force: whether it is attractive or repulsive, the magnitude of the effect, and the positions and existence of a trap and antitrap.

PACS numbers: 04.50.-h 11.15.Yc 73.43.-f 78.20.Jq

In 1948, Casimir[1] showed that quantum fluctuations of the electromagnetic field cause a force between two perfectly conducting, electrically neutral objects. This has since been extended to other materials[2,3]. Throughout this time, Casimir repulsion between two materials in vacuum has been a long sought after phenomenon[4,5]. There are principally four categories in which repulsion can be achieved: (i) Modifying the dielectric of the intervening medium[4,6,7]; (ii) Pairing a dielectric object and a permeable object[5] (such as with metamaterials[8]); (iii) Using different geometries[9–11]; and (iv) Breaking time-reversal symmetry[12,13]. In this letter, we are concerned with Casimir repulsion in identical time-reversal broken systems. Specifically, we will study how Weyl semimetals with time-reversal symmetry breaking can exhibit Casimir repulsion. The key ingredient to Casimir repulsion in this letter is the existence of a nonzero bulk Hall conductance $\sigma_{xy} \neq 0$, $\sigma_{xy} = -\sigma_{yx}$[14].

It is a general theorem that mirror symmetric objects without time-reversal symmetry breaking can only attract one another with the Casimir effect[15]. This is understood with the Lifshitz formula[2] where if we have two materials characterized by the two reflection matrices R_1 and R_2 and separated by a distance a in a parallel plate geometry, we have

$$E_c(a) = \hbar \int \frac{d^2k}{(2\pi)^2} \int \frac{d\omega}{2\pi} \operatorname{tr} \log[\mathbb{I} - R_1 R_2 e^{-2q_z a}], \quad (1)$$

where the trace is a matrix trace and $q_z = \sqrt{\omega^2 + k^2}$. This integral generally yields an attractive force; however, if we break time reversal symmetry, obtaining antisymmetric off-diagonal terms in the reflection matrix $R_{xy} = -R_{yx}$ there is the possibility of Casimir repulsion[16]. One candidate is a two-dimensional Hall material[12], and similarly, another is a topological insulator where the surface states have been gapped by a magnetic field[13,17]. A Hall conductance does not guarantee repulsion; longitudinal conductance can overwhelm any repulsion from the Hall effect (though the magnetic field can lead to interesting transitions[18]), and a Hall effect that is too strong can suppress Kerr rotation and hence lead to attraction. The latter case is an interesting phenomenon where "more" of a repulsive material can lead to attraction.

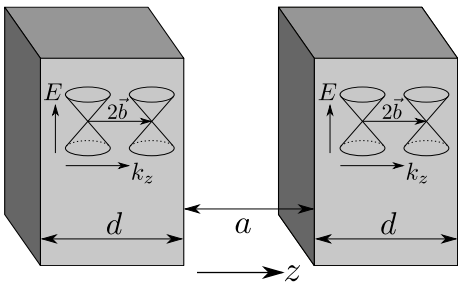

FIG. 1. The setup we will consider here is two Weyl semimetals separated by a distance a in vacuum, and with distance between Weyl cones $2\mathbf{b}$ in k-space (split in the z-direction).

The material we are interested in is marginal in both the case of longitudinal conductance and an overwhelming Hall effect: Weyl semimetals[14] with the Casimir setup seen in Fig. 1 and resulting normalized Casimir pressure in Figs. 2, 3, and 4. These materials have linearly dispersive band structure characterized by Weyl nodes with different chiralities and characterized by a chiral anomaly[19]. Clean Weyl semimetals at zero temperature have a zero DC longitudinal conductivity and optical conductivity $\mathrm{Re}[\sigma_{xx}] \propto \omega$[20]. Additionally, they exhibit a bulk Hall effect exemplified in the DC limit by an axionic field theory[21] where in addition to the Maxwell action, we have

$$S_A = \frac{e^2}{32\pi^2\hbar c} \int d^3r\, dt\, \theta(\mathbf{r}, t) \epsilon^{\mu\nu\alpha\beta} F_{\mu\nu} F_{\alpha\beta}, \quad (2)$$

where $\theta(\mathbf{r}, t) = 2\mathbf{b} \cdot \mathbf{r} - 2b_0 t$, and $2\mathbf{b}$ is the distance between Weyl nodes in $\mathbf{k}$-space while $2b_0$ is their energy offset; e is the charge of an electron; $\hbar$ is Planck's constant; c is the speed of light; $F_{\mu\nu}$ is the electromagnetic

field strength tensor; and $\epsilon^{\mu\nu\alpha\beta}$ is the fully antisymmetric 4-tensor. Inversion symmetry breaking Weyl semimetals, on the other hand, do not exhibit a DC Hall effect[22] and therefore will not see the effects described in this letter. The electrodynamics of this were investigated in[23] where the authors even comment on the possibility for a repulsive Casimir effect.

The marginal nature of Weyl semimetals makes them prime candidates for tuning the Casimir force between attractive and repulsive regimes. In constructed Weyl semimetals made of heterostructures of normal and topological insulators[24] an external magnetic field can control Hall effect[25] and hence the repulsive effects. Additionally, some of the first materials that have been predicted were pyrochlore iridates[26]; these could also see a repulsion tunable with carrier doping or an additional magnetic field.

In a real material and experiment at finite temperature, disorder and interactions should be taken into account and in Weyl semimetals they lead to a finite DC conductivity[20,24,27]. We simulate this effect in the latter part of this letter by raising the chemical potential in our clean system, leading to intraband transitions that contribute to the longitudinal conductivity (in the DC limit these are singular contributions).

To begin, we consider two semi-infinite slabs of Weyl semimetal ($z < 0$ and $z > a$ to be precise), neglecting all frequency dependence to the conductivities by assuming the electromagnetic response is captured by Eq. (2). The result is just a material that is solely a bulk Hall material with current responses given by the Hall conductivity $\sigma_{xy} = e^2 b/2\pi^2\hbar$. This response can be encoded in the dielectric function so that $\epsilon_{xx} = \epsilon_{yy} = \epsilon_{zz} = 1$ and $\epsilon_{xy} = -\epsilon_{yx} = i\sigma_{xy}/\omega$. With this set up, if an incident wave $\mathbf{k}$ hits such a material it will break up into two different polarizations in the material $\mathbf{k}^\pm$ that satisfy $k_x^\pm = k_x$, $k_y^\pm = k_y$, and $(k_z^\pm)^2 = k_z(k_z \pm \sigma_{xy}/c)$. Additionally, the two elliptical polarizations $\mathbf{D}_\pm = \epsilon(\omega)\mathbf{E}_\pm$ are $\mathbf{D}_\pm \propto \frac{\omega}{ck^\pm}(k_z \pm \sigma_{xy}/c)\mathbf{e}_1 \mp ik_z^\pm \mathbf{e}_2$ where $\mathbf{e}_2$ is perpendicular to the plane of incidence and $\mathbf{e}_1 = \mathbf{e}_2 \times \mathbf{k}^\pm$. Notice that for $k_z < \sigma_{xy}/c$, one of the polarizations is evanescent.

The incident and reflected polarizations can be broken up into transverse electric (TE) and transverse magnetic (TM) modes, and the reflection matrix $R(\omega, \mathbf{k})$ just connects incident to reflected $(E_r^{\mathrm{TM}}, E_r^{\mathrm{TE}})^T = R(\omega, \mathbf{k})(E_0^{\mathrm{TM}}, E_0^{\mathrm{TE}})^T$. As shown in the Lifshitz formula Eq. (1), we need the imaginary frequency reflection matrix. If we let $\omega \to i\omega$ and define $q_z^2 = \omega^2/c^2 + k_x^2 + k_y^2$, the reflection matrix for a semi-infinite slab of this bulk Hall material as

$$R_\infty(iq_z) = \frac{1}{\sigma_{xy}/c}\begin{pmatrix} Q_- - \sigma_{xy}/c & -Q_+ + 2q_z \\ Q_+ - 2q_z & Q_- - \sigma_{xy}/c \end{pmatrix}, \quad (3)$$

where we have defined for brevity $Q_\pm = \sqrt{2q_z(\sqrt{q_z^2 + \sigma_{xy}^2/c^2} \pm q_z)}$ (the real frequency version of R_∞ is found in the supplement[28]). Inspecting $R_\infty(iq_z)$, we see that the reflection matrix only depends on the ratio cq_z/σ_{xy}. This dependence has implications for the Casimir force. After changing variables to solely q_z, we can inspect the Casimir pressure $P_c(a) = -\partial E_c/\partial a$, and we have an expression $P_c = \frac{2\hbar c}{(2\pi)^2}\int dq_z\, q_z^3 \;\; g\left[\frac{q_z}{\sigma_{xy}/c}, 2q_z a\right]$, with a function $g(\frac{q_z}{\sigma_{xy}/c}, 2q_z a)$ written out in the supplement[28] for completeness. If we then change variables to $x = 2aq_z$ and normalize by Casimir's original result for perfect conductors $P_0 = -\frac{\hbar c\pi^2}{240a^4}$[1], we can write the equation for the pressure as $P_c/P_0 = f(\sigma_{xy}a/c)$.

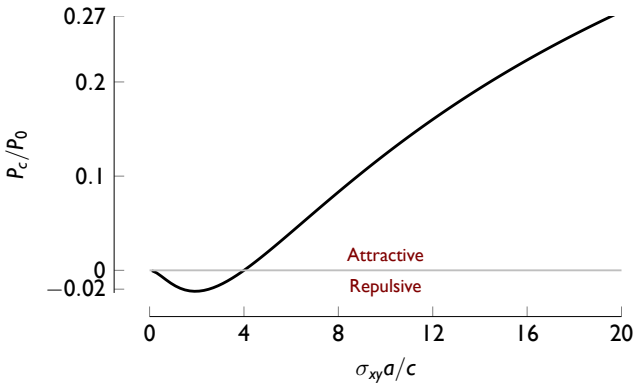

FIG. 2. The normalized Casimir force between two semi-infinite bulk Hall materials. Repulsion is seen for $\sigma_{xy}a/c \lesssim 4.00$. P_0 is the distant-dependent ideal Casimir Force[1]. For $\sigma_{xy}a/c \to \infty$, $P_c/P_0 \to 1$.

With this formulation, we plot normalized force P_c/P_0 as a function of $\sigma_{xy}a/c$ obtaining the single function seen in Fig. 2. We see that for $\sigma_{xy}a/c \lesssim 4.00$ we obtain repulsion while for $\sigma_{xy}a/c \gtrsim 4.00$ we obtain attraction. Thus, these similar materials trap each other at a fixed distance simply dependent on the Hall conductivity, $a_{\mathrm{Trap}} \approx \frac{4.00}{\sigma_{xy}/c}$. If we insert the value of $\sigma_{xy} = e^2 b/2\pi^2\hbar$ into this expression, we find $a_{\mathrm{Trap}} \approx 860/b$. This means that if $1/b \sim O(\mathrm{nm})$, then $a_{\mathrm{Trap}} \sim O(\mu\mathrm{m})$ quite reasonable.

As the distance between the materials gets large, $P_c/P_0 \to 1$. This behavior is markedly different from the thin film Hall case obtained by Tse and MacDonald in[12,17]. They found a small (two-dimensional) quantum Hall effect implies a quantized and repulsive Casimir force at large distance. In our case, we get attraction at large distances for a bulk Hall material independent of the magnitude of the Hall effect. To resolve this seeming inconsistency, imagine a finite thickness of the bulk Hall material of thickness d, then the two-dimensional conductivity $\sigma_{xy}d$ diverges as $d \to \infty$, and in the case of a 2D quantum Hall plate with infinite Hall conductivity, the Casimir effect is attractive and approaches P_0.

To make this argument more precise, one can actually find the reflection matrix for a bulk Hall system of thickness d and the result is (derivation of R_d depends only on the axionic action Eq. (2) and can be found in the

supplement[28], calculated for real frequencies)

$$R_d(iq_z) = \begin{pmatrix} R_{xx} & R_{xy} \\ -R_{xy} & R_{xx} \end{pmatrix}, \tag{4}$$

with

$$R_{xx} = -\tfrac{1}{2}\tfrac{\sigma_{xy}}{c}(Q_- \sinh Q_+ d + \tfrac{\sigma_{xy}}{c}\cosh Q_+ d - Q_+ \sin Q_- d - \tfrac{\sigma_{xy}}{c}\cos Q_- d)/D, \tag{5}$$

$$R_{xy} = -\tfrac{1}{2}\tfrac{\sigma_{xy}}{c}(Q_+ \sinh Q_+ d + 2q_z \cosh Q_+ d - Q_- \sin Q_- d - 2q_z \cos Q_- d)/D, \tag{6}$$

where

$$D = (Q_+^2 + \tfrac{1}{2}\tfrac{\sigma_{xy}^2}{c^2})\cosh Q_+ d + (2q_z Q_+ + \tfrac{\sigma_{xy}}{c}Q_-)\sinh Q_+ d + (Q_-^2 - \tfrac{1}{2}\tfrac{\sigma_{xy}^2}{c^2})\cos Q_- d + (2q_z Q_- - \tfrac{\sigma_{xy}}{c}Q_+)\sin Q_- d. \tag{7}$$

It can be shown that $\lim_{d\to\infty} R_d(iq_z) = R_\infty(iq_z)$.

Similarly, in the limit of $d \to 0$, if we keep $\sigma_{xy}^{\rm 2D} = \sigma_{xy} d$ constant, we obtain what was found in[12]

$$\lim_{d\to 0} R_d(iq_z) = \frac{1}{1+(\sigma_{xy}^{\rm 2D}/2c)^2}\begin{pmatrix} -(\sigma_{xy}^{\rm 2D}/2c)^2 & -\sigma_{xy}^{\rm 2D}/2c \\ \sigma_{xy}^{\rm 2D}/2c & -(\sigma_{xy}^{\rm 2D}/2c)^2 \end{pmatrix}.$$

For the rest of our discussion, define $R_0(iq_z) = \lim_{d\to 0} R_d(iq_z)$ with $\sigma_{xy}^{\rm 2D} = \sigma_{xy} d$ held constant.

With the correct limits identified, we first notice that we can write R_d as a function of only two variables $R_d = R_d(cq_z/\sigma_{xy}, \sigma_{xy}^{\rm 2D}/c)$. Thus, by similar arguments to what we had for the semi-infinite case, the Casimir pressure $P_c = P_0 f(\sigma_{xy} a/c, \sigma_{xy}^{\rm 2D}/c)$.

The limiting cases can be understood now by considering first Eq. (1). The exponential constrains $q_z \sim 1/a$ and since technically the "thin-film" limit is $\lim_{q_z d\to 0} R_d(iq_z) = R_0(iq_z)$, we have that $d/a \to 0$. In other words, the thin film limit is applicable when we are considering $d \ll a$. The opposite limit is just when $q_z d \to \infty$, and by similar arguments, that means $d \gg a$ is when the semi-infinite case applies. Both limits leave $\sigma_{xy} a/c$ and $\sigma_{xy} d/c$ unaffected (though in the thin film case $\sigma_{xy} a$ drops out while in the semi-infinite case $\sigma_{xy} d \to \infty$ has the same limit as $q_z d \to \infty$).

The thin film limit can be evaluated exactly[12] and has the form $P_c^{\rm TF} = P_0 \frac{90}{\pi^4}\,{\rm Re}\{{\rm Li}_4\left[(\sigma_{xy}^{\rm 2D}/c)^2/(\sigma_{xy}^{\rm 2D}/c + 2i)^2\right]\}$ where $\rm Li_4$ is the polylogarithm of degree 4. Note that this function has a minimum value of $P_c^{\rm TF} \approx -0.117 P_0$ representing how repulsive we can get. For large enough $\sigma_{xy}^{\rm 2D}/c$, the force does become attractive—corresponding roughly to when $(\sigma_{xy}^{\rm 2D}/c)^2 > \sigma_{xy}^{\rm 2D}/c$ (i.e. when Kerr rotation is suppressed).

The cross-over between these regimes can be seen in Fig. 3. As $\sigma_{xy} d/c$ is increased, the Casimir energy approaches the semi-infinite case. However, for any finite d, each curve asympotically approaches its thin-film value (and never goes lower than the minimum value represented by dashed horizontal line in Fig. 3). This not only clearly connects our case to the previously known thin-film result, it also provides a theoretical justification for considering a thin-film limit $d \ll a$ with a two-dimensional conductance $\sigma_{\mu\nu} d$.

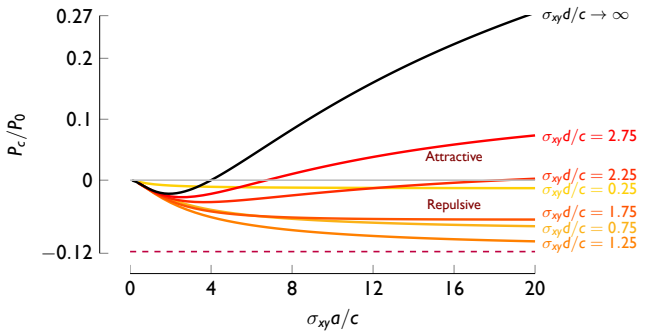

FIG. 3. (Color online) A plot of the normalized Casimir force for various thicknesses of a bulk Hall material (idealized Weyl semimetal). It begins slightly repulsive for small $\sigma_{xy} d/c$, and as this increases, it becomes more repulsive until it reaches the maximum for a thin film material (the dashed line) at which point it increases to the semi-infinite limit. $P_0 = -\frac{\hbar c \pi^2}{240 a^4}$ and $\sigma_{xy} = e^2 b/2\pi^2\hbar$ is the bulk Hall response. Fig. 4 takes into account more material properties.

Until now the plates have been idealized. Using the thin film limit illustrated above as a reference allows us to easily consider some of the effects of taking into account the full frequency response of the material. Thus, we pick a $\sigma_{xy} d$ that is reasonably in the repulsive regime (for all distances) in order to analyze the effects of including some of the lowest order frequency dependence into the conductivities. We will mainly be interested in the effects of virtual vacuum transitions that are low in energy, which corresponds to plates that are far apart from one another. Thus, we will use the low-energy chiral Hamiltonian for a pair of Weyl nodes

$$H_W = \pm\hbar v_{\rm F} \boldsymbol{\sigma}\cdot(\mathbf{k} \pm \mathbf{b}), \tag{8}$$

where $v_{\rm F}$ is the Fermi velocity and $\mathbf{b}$ is the position of the

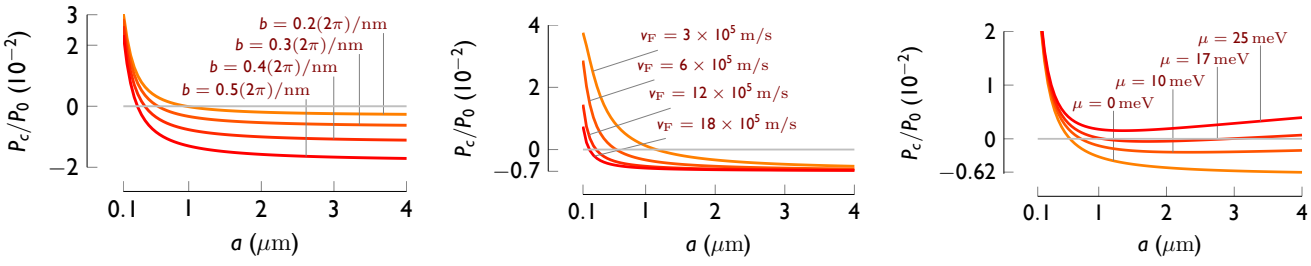

(a) (b) (c)

FIG. 4. The Casimir force for a thin film Weyl semimetal taking into account low-energy virtual transitions in the band structure. An anti-trap develops when the longitudinal conductivity overwhelms the Hall conductivity. In (a) we compare different values of b (or equivalently, changing the Hall effect); in (b) we compare different v_F (the larger v_F the smaller σ_{xx} is); and in (c) we turn on a finite chemical potential which causes attraction at very large distances (and hence a trap). Even small chemical potentials have this property but the trap is quite far out. Unless the parameter is varying, $a_0 = 1\,\text{nm}$, $d = 20\,\text{nm}$, $b = 0.3(2\pi/a_0)$, $\Lambda = 2\pi/a_0$, $v_F = 6 \times 10^5\,\text{m/s}$, and $\mu = 0$.

of Weyl node in $\mathbf{k}$-space. The exact band structure will be important as the plates get closer though weighting will still be larger on the lower energy modes.

To the conductivities, we fix k_z and calculate two-dimensional conductivities using the Kubo-Greenwood formulation (see the supplement[28] for details), then integrate the resulting expression over k_z with a symmetric cutoff $\sigma_{\mu\nu}(i\omega) = \int_{-\Lambda}^{\Lambda} \frac{dk_z}{2\pi} \tilde{\sigma}_{\mu\nu}(i\omega; k_z)$[29] where $\tilde{\sigma}_{\mu\nu}(i\omega; k_z)$ is the two-dimensional conductivity with k_z fixed. We evaluate this at imaginary frequency to aid the Casimir calculations.

We perform this procedure at finite chemical potential μ and throw out terms that go to zero when the cutoff $\Lambda \to \infty$. This yields the conductivities

$$\sigma_{xx}(i\omega) = \frac{e^2}{12\pi^2\hbar v_F}\left[\tfrac{5}{3}\omega + 2\omega\log\left(\tfrac{v_F\Lambda}{\omega}\right) + 4\tfrac{\mu^2}{\hbar^2\omega} - \omega\log\left(1+\tfrac{4\mu^2}{\hbar^2\omega^2}\right)\right], \quad (9)$$

and $\sigma_{xy}(i\omega) = \frac{e^2 b}{2\pi^2\hbar}$ is unchanged at this order. Due to the linear dispersion of the Weyl nodes, we have a logarithmic cutoff dependence. Note that rotating to real frequencies we get the correct result for two Weyl nodes for $\text{Re}[\sigma_{xx}(\omega)]$[20], and a result with the appropriate logarithmic divergence for $\text{Im}[\sigma_{xx}(\omega)]$[30]. This can be understood in terms of charge renormalization due to the band structure, but for ease of our purposes we let $\Lambda \sim 1/a_0$ where a_0 is the lattice spacing. For our plots we choose a lattice spacing of $a_0 = 1\,\text{nm}$, a thickness of $d = 20\,\text{nm}$, $b = 0.3(2\pi/a_0)$, $\Lambda = 2\pi/a_0$, $v_F = 6 \times 10^5\,\text{m/s}$, and $\mu = 0$ unless its the parameter we are varying.

Now, one can use one of two equivalent ways of calculating the Casimir energy: the reflection matrix as given in[12], or using a microscopic analysis to find the photon dressed RPA current-current correlators[28]. In order to avoid an unphysical negative $\sigma_{xx}(i\omega)$ as well as for consistency, we cutoff the photon energies in the Lifshitz formula to run from 0 to Λ—an approximation valid for $a \gg \frac{c}{v_F}\Lambda^{-1}$.

First, we see that we get an anti-trap for these at approximately 650 nm, and if we increase b as in Fig. 4a (with, say, an applied magnetic field), it not only moves closer to zero separation, but the overall repulsive behavior can be enhanced. On the other hand, if we increase v_F as we see in Fig. 4b, we see the region of attraction is suppressed, but the overall repulsive behavior at large distances is maintained. Modifying Λ will have effects similar to modifying v_F, but since it appears logarithmically, it would need to change by orders of magnitude to give appreciable changes (a simple plot for this is provided in the supplement, but is not relevant for the discussion here). This "anti-trap" effect is occurring at short distances when higher order band effects also play a role, but any other effects will contribute to the longitudinal conductivity in such a way that an anti-trap will appear.

Interestingly, when we introduce a finite chemical potential as we see in Fig. 4c. In addition to the anti-trap we get at shorter distances, we start to see a trap at much longer distances appear. This is not surprising since at zero frequency there is a divergent longitudinal conductivity. Thus, we know that at long distances, the Casimir force must be attractive, but by modifying the Hall effect, we have an intermediate regime of repulsion. A similar effect would occur if we took finite temperature or disorder corrections to the longitudinal conductivities.

Considering the form of the conductance in terms of the fine structure constant, $\sigma_{xy}d/c = \alpha\frac{2bd}{\pi}$, we see that bd controls the strength of the repulsion in the thin film limit. Without longitudinal conductance, the repulsive regime roughly corresponds to when $(\sigma_{xy}d/c)^2 \lesssim \sigma_{xy}d/c$ or equivalently $\frac{2bd}{\pi} \lesssim \frac{1}{\alpha}$. The longitudinal conductance introduces v_F into the scheme; relevant photons have $\omega \approx c/a$ and thus it becomes important for $\sigma_{xx}d/c \sim \alpha\frac{c}{v_F}\frac{d}{a} \gtrsim O(1)$ (neglecting constants) which both emphasizes that v_F controls the longitudinal conductance's contribution to the Casimir effect and that the term is suppressed at longer distances.

We have shown here how Weyl semimetals can exhibit

a tunable repulsive Casimir force (with, for instance, magnetic field tuning **b**) and how it can depend on the thickness of the material. In the thin film limit, we showed how the semimetalic nature of these materials can work to create attraction at smaller distances scales, and how a finite longitudinal conductivity will create long distance attraction along with repulsion at intermediate distances. Recently the first experimental observation of Weyl semimetals[31,32] provides optimism that these theoretical materials could be a reality. The marginal nature of these materials could be useful for controlling the Casimir force between attractive and repulsive regimes.

Acknowledgements – This work was supported by the DOE-BES (Grant No. DESC0001911) (A.A. and V.G.), the JQI-PFC (J.W.), and the Simons Foundation. We thank Liang Wu and Mehdi Kargarian for discussions.

[1] H. B. G. Casimir, Proc. K. Ned. Akad. Wet. **51**, 793 (1948).
[2] E. M. Lifshitz, Sov. Phys. JETP **2**, 73 (1956).
[3] M. Bordag, U. Mohideen, and V. M. Mostepanenko, Phys. Rep. **353**, 1 (2001).
[4] I. E. Dzyaloshinskii, E. M. Lifshitz, and L. P. Pitaevskii, Sov. Phys. Usp. **4**, 153 (1961).
[5] T. H. Boyer, Phys. Rev. A **9**, 2078 (1974).
[6] O. Kenneth, I. Klich, A. Mann, and M. Revzen, Phys. Rev. Lett. **89**, 033001 (2002).
[7] J. N. Munday, F. Capasso, and V. A. Parsegian, Nature **457**, 170 (2009).
[8] U. Leonhardt and T. G. Philbin, New J. Phys. **9**, 254 (2007); F. S. S. Rosa, J. Physics: Conf. Series **161**, 012039 (2009).
[9] T. H. Boyer, Phys. Rev. **174**, 1764 (1968).
[10] S. A. Fulling, L. Kaplan, and J. H. Wilson, Phys. Rev. A **76**, 012118 (2007).
[11] M. Levin, A. P. McCauley, A. W. Rodriguez, M. T. H. Reid, and S. G. Johnson, Phys. Rev. Lett. **105**, 090403 (2010).
[12] W. K. Tse and A. H. MacDonald, Phys. Rev. Lett. **109**, 236806 (2012).
[13] A. G. Grushin and A. Cortijo, Phys. Rev. Lett. **106**, 020403 (2011).
[14] P. Hosur and X. Qi, C. R. Phys. **14**, 857 (2013).
[15] O. Kenneth and I. Klich, Phys. Rev. Lett. **97**, 160401 (2006).
[16] G. L. Klimchitskaya, U. Mohideen, and V. M. Mostepanenko, Rev. Mod. Phys. **81**, 1827 (2009).
[17] P. Rodriguez-Lopez and A. G. Grushin, Phys. Rev. Lett. **112**, 056804 (2014).
[18] A. A. Allocca, J. H. Wilson, and V. Galitski, Phys. Rev. B **90**, 075420 (2014).
[19] V. Aji, Phys. Rev. B **85**, 241101 (2012).
[20] P. Hosur, S. A. Parameswaran, and A. Vishwanath, Phys. Rev. Lett. **108**, 046602 (2012).
[21] A. A. Zyuzin and A. A. Burkov, Phys. Rev. B **86**, 115133 (2012).
[22] G. B. Halász and L. Balents, Phys. Rev. B **85**, 035103 (2012).
[23] A. G. Grushin, Phys. Rev. D **86**, 045001 (2012).
[24] A. A. Burkov and L. Balents, Phys. Rev. Lett. **107**, 127205 (2011).
[25] Y. Chen, S. Wu, and A. A. Burkov, Phys. Rev. B **88**, 125105 (2013).
[26] X. Wan, A. M. Turner, A. Vishwanath, and S. Y. Savrasov, Phys. Rev. B **83**, 205101 (2011); G. Chen and M. Hermele, *ibid.* **86**, 235129 (2012); W. Witczak-Krempa and Y. B. Kim, *ibid.* **85**, 045124 (2012).
[27] A. A. Burkov, M. D. Hook, and L. Balents, Phys. Rev. B **84**, 235126 (2011).
[28] See Supplemental Material at [URL will be inserted by publisher] for calculational details.
[29] P. Goswami and S. Tewari, Phys. Rev. B **88**, 245107 (2013).
[30] B. Rosenstein and M. Lewkowicz, Phys. Rev. B **88**, 045108 (2013).
[31] S.-M. Huang, S.-Y. Xu, I. Belopolski, C.-C. Lee, G. Chang, B. Wang, N. Alidoust, G. Bian, M. Neupane, A. Bansil, H. Lin, and M. Z. Hasan, "An inversion breaking Weyl semimetal state in the TaAs material class," (2015), arXiv:1501.00755.
[32] C. Zhang, S.-Y. Xu, I. Belopolski, Z. Yuan, Z. Lin, B. Tong, N. Alidoust, C.-c. Lee, S.-m. Huang, H. Lin, M. Neupane, D. S. Sanchez, H. Zheng, G. Bian, J. Wang, C. Zhang, T. Neupert, M. Z. Hasan, and S. Jia, "Observation of the Adler-Bell-Jackiw chiral anomaly in a Weyl semimetal," (2015), arXiv:1503.02630.